Influence of Nanoclay on the Rheological Properties of Polyamide 6/Acrylonitrile Butadiene Styrene Nanocomposites

Alireza Mojarrad, Yousef Jahani, Mehdi Barikani

Iran Polymer and Petrochemical Institute, P.O. Box 14185-458, Tehran, Iran

Received 14 August 2010; accepted 4 January 2011
DOI 10.1002/app.34092
Published online 2 February 2012 in Wiley Online Library (wileyonlinelibrary.com).

ABSTRACT: The objective of this paper is to study the influence of nanoclay on rheological behavior and phase morphology of immiscible polyamide 6/acrylonitrile butadiene styrene (PA6/ABS) blends. For this purpose, the rheological behavior of PA6/ABS/Nanoclay blends such as storage modulus, relaxation time mechanism, zero-shear viscosity, interfacial relaxation time, relaxation modulus, interface modulus, and the relationship between rheology and morphology was investigated. It was observed that the relaxation time (λ) and zero-shear viscosity (η_0) increases by increasing of the nanoclay (2–6 wt %) and ABS (15–35 wt %) content. As, the increase in relaxation time of PA6/ABS/Nanoclay blends with increasing of the nanoclay explained through deformation of droplets and the physical interactions across the interface that causes to enhancement of elasticity behavior at low frequencies. In other words, this occurrence causes the relaxation time slightly shifted toward higher values by increasing of nanoclay loading. The relaxation time spectrum caused by the interfacial tension of the droplets can be calculated by subtracting the contribution of the components from the nanocomposite spectrum reported by Gramespacher and Meissner. The results of the study show that the nanoclay localization in blend can be suggested from $H(\lambda)\lambda_{interface}$ as a function of relaxation time diagram which nanoclay plates located in matrix, disperse phase, or interphase. In addition, the slopes of relaxation modulus curves decrease by increasing nanoclay and ABS weight fraction, indicating that the relaxation time increases with the addition of nanoclay. © 2012 Wiley Periodicals, Inc. J Appl Polym Sci 125: E571–E582, 2012

Key words: PA6/ABS/Nanoclay blends; relaxation time spectrum; interfacial relaxation time; relaxation modulus; interfacial modulus

INTRODUCTION

In nano-filled blends, investigation of the rheological behavior is the most important way to find out the level of polymer–filler interactions and the structure–property relationship.[1–6] Study of the rheological properties can be an interesting method to quantify the evolution of phase morphology and nanoclay dispersion in polymer blends during flow.[7,8] Adding nanoparticles to polymer blends will typically affect the nonlinear and time dependent properties. In this case, Hong et al.[9] reported that the adding nanoclay to an immiscible polymer blends stabilizes the phase morphology due to the compatibilization effect.[10,11] They described that the nanoclay located at the interface forms the interfacial phase along the interface and changes the interfacial tension, which result in the coalescence suppression of the dispersed droplets. In other work, Hong et al.[12] investigated the interfacial tension reduction in polybutylene terephthalate (PBT)/polyethylene (PE)/Clay blend, and the results showed that the nanoclay located at the interface significantly influences alter in the phase morphology such as droplet size and droplet size distribution.[13] These morphological changes are caused by the compatibilization effect of nanoclay involved in the interfacial tension reduction.[9] In particular, study of stress relaxation can obtain interesting information about the evolution of phase morphology.[14–20] It was observed that the stress relaxation modulus curves of blends presented two steps: a fast relaxation, which can be related to the contribution of the relaxation of the pure components, and a slower relaxation, was attributed to the relaxation of the deformed droplets. Similar results by Yee et al.,[21] Okamoto et al.,[15] Iza and Bousmina,[16] and Takahashi et al.[22] were obtained for *Polystyrene*/Polycarbonate(*PS/PC*) polyisobutylene/polydimethylsiloxane (PIB/PDMS), and PIB/PDMS blends, respectively.

The relaxation mechanism associated with the deformation of dispersed droplets in a matrix as reported by Gramespacher and Meissner,[23] Bousmina and Muller,[24] and Lacroix et al.[25] The relationship between the relaxation spectrum $H(\lambda)$ and dynamic modulus G' and G'' can be expressed through the neural network model and a modified Tikhonov regularization method developed by Honerkamp and Weese[26] using the following eqs. (1) and (2)[27,28]:

Correspondence to: M. Barikani (M.Barikani@ippi.ac.ir).

TABLE I
Composition of the Investigated Blends

Formulation	Constituents			
Compatibilized ternary blends	PA6	ABS	EnBACO-MAH	Nanoclay
PA6/ABS/ EnBACO-MAH/Nanoclay	80	15	5	0
PA6/ABS/ EnBACO-MAH/Nanoclay	60	35	5	0
PA6/ABS/ EnBACO-MAH/Nanoclay	80	15	5	2
PA6/ABS/ EnBACO-MAH/Nanoclay	80	15	5	4
PA6/ABS/ EnBACO-MAH/Nanoclay	80	15	5	6
PA6/ABS/ EnBACO-MAH/Nanoclay	70	25	5	2
PA6/ABS/ EnBACO-MAH/Nanoclay	70	25	5	4
PA6/ABS/ EnBACO-MAH/Nanoclay	70	25	5	6
PA6/ABS/ EnBACO-MAH/Nanoclay	60	35	5	2
PA6/ABS/ EnBACO-MAH/Nanoclay	60	35	5	4
PA6/ABS/ EnBACO-MAH/Nanoclay	60	35	5	6

$$G'(\omega) = \int_0^\infty H(\lambda) \frac{(\omega\lambda)^2}{1+(\omega\lambda)^2} \frac{d\lambda}{\lambda} \quad (1)$$

$$G''(\omega) = \int_0^\infty H(\lambda) \frac{\omega\lambda}{1+(\omega\lambda)^2} \frac{d\lambda}{\lambda} \quad (2)$$

where $H(\lambda)$ is the continuous relaxation spectrum and λ is the relaxation time. Also, the relaxation spectrum ($H(\lambda)$) can be determined through Tschoegle approximation[29] as exposed in eq. (3):

$$H(\lambda) = G' \left[\frac{d\lg G'}{d\lg\omega} - \frac{1}{2}\left(\frac{d\lg G'}{d\lg\omega}\right)^2 - \frac{1}{4.606}\left(\frac{d^2\lg G'}{d(\lg\omega)^2}\right) \right]_{1/\omega=\lambda/\sqrt{2}} \quad (3)$$

Using the continuous demonstration of the Maxwell model, the relaxation spectrum $H(\lambda)$ is related to G' and G'' through the Fred Holm integral equation of the first kind.[27] A method suggested by Gramespacher and Meissner[23] consists of plotting the relaxation time spectrum $H(\lambda)\lambda$ as a function of λ and using the position of the maximum in the resulting curve as the relaxation time for the droplets.

The objective of this paper is to report the influence of the nanoclay addition on the rheological properties and phase morphology of polyamide 6/acrylonitrile butadiene styrene (PA6/ABS) blends. For this purpose, blends based on the PA6/ABS/Nanoclay with different compositions from PA6, ABS, and nanoclay were prepared. We have investigated the rheological properties of PA6/ABS/Nanoclay blends such as mechanism of relaxation time, relaxation modulus, interface modulus, and the relationship between the rheological behaviors of the blends and their morphologies. In addition, finding out a correlation between relaxation time, relaxation modulus, interface modulus, and elasticity behavior was the center of this study.

EXPERIMENTAL

Materials

All materials used in this work are supplied from commercial sources. PA6 with trade name Ultramid B3S HP with a density of 1.13 g cm^{-3}, and a melt flow index (MFI at 275°C and 5 kg loading) of 175 g/10 min was supplied commercially from BASF Company. ABS with trade name SD 0150 with a density of 1.17 g cm^{-3}, and a MFI (200°C, 5 kg; ASTM D1238) of 1.40–2.20 g/10 min was obtained commercially from Tabriz Petrochemical Company. EnBACO-MAH (ethylene-n butyl acrylate-carbon monoxide-maleic anhydride) as compatibilizer was provided by DuPont with trade name Fusabond® A MG423D (Ethylene Acrylate Terpolymer) with specifications of MFI (190°C, 2.16 kg): 8 g/10 min, melting point: 62°C and MAH content: 16.6 mg KOH/g. Nanoclay having a cation exchange capacity of 90 mequiv/100 g, with trade name of Cloisite® C30B with density and *d*-spacing 1.98 g cm^{-3} and 18.5°A, respectively, was supplied by Southern Clay products Inc.

Preparation of PA6/ABS/Nanoclay blends

Before blend preparation, the components were dried for 16 h in vacuum oven at 85°C. The PA6/ABS/EnBACO-MAH/Nanoclay blends, having different compositions (PA6, ABS, and nanoclay), were melt blended in a twin-screw Brabender Plasticorder with a temperature profile of 235–236–237–238–239–240°C at a screw speed of 80 rpm and feeding ratio of approximately 1 kg h^{-1}. The extrudate was rapidly quenched with cold water and pelletized. The produced pellets were again dried at 85°C for 16 h before injection molding. The barrel zone temperatures of the injection molder were set at 240, 245, and 240°C. Detailed compounding formulations of PA6/ABS/EnBACO-MAH/Nanoclay blends for this study have been shown in Table I.

Characterization of blend morphologies

Droplet sizes have been observed by scanning electron microscopy (SEM) using a VEGA TESCAN model. Before morphological observations, samples were first fractured in liquid nitrogen. PA6 and ABS phases were etched by immersing the fracture surfaces in tetra hydro furan (THF) for 72 h at room temperature to remove the dispersed phase domains. Later, it was dried for 24 h in a vacuum oven at 80°C and then gold sputtered. The microscopy operating at 20 kV was used to view the specimens, and several microscopy photographs were taken for each sample.

Rheological measurements

Dynamic rheological measurements were conducted with a MCR 300-Physica rheometer using a parallel plate system with plate of diameter 25 mm. Frequency sweeps were performed over the range of 0.01–600 rad s^{-1} at 245°C. All experiments were carried out at a temperature of 245°C, under a continuous purge of dry nitrogen, to suppress the oxidative degradation process of melts at high temperatures and absorption of moisture. Experimentally, in a rotational rheometer, the test was carried out to determine the linear viscoelastic limit consists in the evaluation of the viscoelastic parameters as a function of the strain at a fixed frequency (strain sweep tests). Moreover, to gain information about relaxation behavior of the blends, stress relaxation tests have been carried under a steady strain amplitude ($\gamma = 10\%$) at 245°C.

RESULTS AND DISCUSSION

Characterization of PA6/ABS/Com/Nanoclay nanocomposites

Figure 1 shows the small-angle X-ray scattering (SAXS) patterns of nanoclay and nano-filled blends

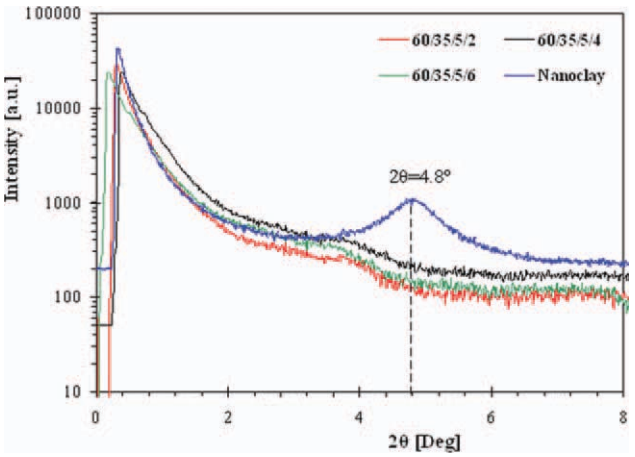

Figure 1 SAXS patterns of nanoclay and blends with 2, 4, and 6 wt % nanoclay. [Color figure can be viewed in the online issue, which is available at wileyonlinelibrary.com.]

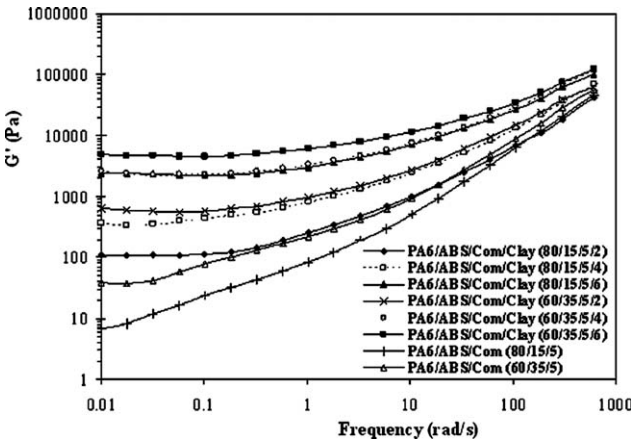

Figure 2 Storage modulus versus frequency for the PA6/ABS/Com/Clay blends at 245°C.

in the region of $2\theta = 2$–$10°$. As shown in Figure 1, the nanoclay exhibits the first characteristic peak at 4.89°, corresponding to a *d*-spacing of 1.8 nm. This demonstrates that basal spacing of the layered silicates increased due to the insertion of polymer chains into the layer silicates. In the case of the blends, the characteristic peak of the nanoclay almost disappears, and the second peak regarding to the blends is almost no longer observed. These results indicate that the PA6 and ABS chains have penetrated into the silicate gallery, and the nanoclay platelets mostly exfoliated in the PA6 matrix and ABS dispersed phase and/or interface. It suggests that the internal structure of the layered silicates is mainly decided by the intercalation of PA6 and ABS chains into nanoclay galleries. This can be explained by the competitive interaction between polymers with nanoclay particles. Also, the reduction of the scattering intensity indicates that the nanoclay structure becomes relatively exfoliated by the polymer chains. The characteristic SAXS are detected in the blends, indicating that the degree of layered silicates exfoliation in all the blends is similar to each other. Hence, the relatively degree of exfoliation resulted in a significant decrease in the dispersed droplets size.

Dynamic rheology

The storage modulus (G') as a function of frequency in the linear viscoelastic region for PA6/ABS/Com/Nanoclay blends at 245°C containing different amounts of nanoclay (2, 4, and 6 wt %) and ABS (15, 25, and 35 wt %) is illustrated in Figure 2. According to Figure 2, the amount of the storage modulus for all of the nano-filled blends increases with the addition of nanoclay and ABS content especially at low frequency region. The storage modulus curves of different blends, which are in all of the frequency

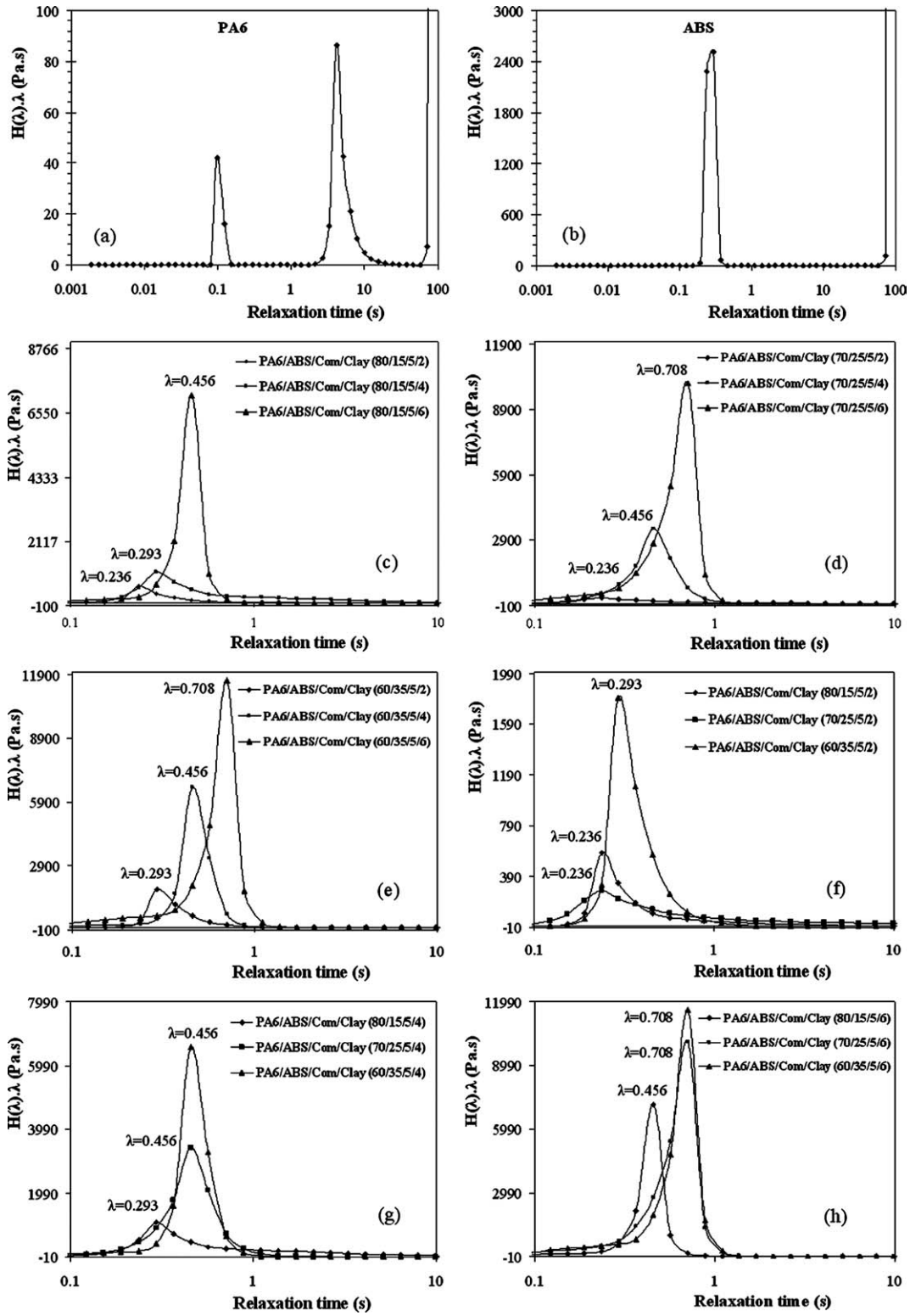

Figure 3 Relaxation time spectra of PA6/ABS/Com/Nanoclay blends of varying nanoclay and ABS contents at 245°C.

region, show similar trend, and plateau can be observed for all the blends at low frequencies region. The effect of nanoclay is especially apparent plateau at low frequencies of the storage modulus, which is characteristic of blends exhibiting solid-like behavior.[30,31] In the most cases, the solid-like behavior due to the increased of nanoparticle–polymer interaction will lead to a larger extent exfoliation of nanoparticles in the blends. Hence, the solid-like behavior indicates strong interactions between the filler and polymer phase.[32,33] Consequently, the increase of elasticity in the low frequency region is originated

from the strong interaction between component and nanoparticle.[34] Thus, it seems that the amount of nanoclay has a significant effect in the elasticity of the interfaces. Since the dynamic modulus is directly related to the size of the drops, this suggests that the drop size does decrease upon increasing nanoclay loading. Conversely, this observation suggests that, at higher frequencies, the incorporation of nanoclay do not significantly affect the dynamics of the PA6 chains. At these frequencies, by increasing nanoclay content, the storage modulus is observed to increase, which can be attributed to an increased effective deformation rate in the matrix (PA6). Whereas the study of elastic modulus of the blends at low frequency provides further evidence of the morphological changes. Therefore, the low frequency modulus mainly gives information about the aggregates and eventually the percolating structure formed by the aggregates, the high frequency modulus is always dominated by the polymeric matrix contributions.[31] This contribution of the interfacial tension to the storage modulus is increased by the increased interfacial area with a change in the droplet size.[35] Moreover, Huitric et al.[10] have shown that the addition of nanoclay leads to a lower interfacial tension. As, blends with a cocontinuous morphology usually display a power law-like relaxation of the elastic modulus at low frequencies region. On the contrary, the increase of volume fraction of the disperse phase leads to an increase of the G' plateau [Fig. 2]. Also, loss modulus (G'') values are not shown because G' is more sensitive to microstructural effects.

Influence of nanoclay on the relaxation time

All of the relaxation spectra were calculated from experimental storage modulus data, using a nonlinear spectrum calculation method, available in MCR-300 rheometer software. The $H(\lambda)\lambda$ as a function of λ in the liner viscoelastic region for PA6/ABS/Com/Nanoclay blends at 245°C containing different amounts of nanoclay (2%, 4%, and 6%) and ABS (15%, 25%, and 35%) is presented in Figure 3(a)–(h). As can be seen the relaxation spectra of PA6 exhibit two peaks and ABS only one peak. In contrast, upon increasing of the nanoclay level to 6 wt %, all of the spectra have a single peak for all of the blends, and the peak slightly shifted toward a longer time. On the other hand, it is observed that the relaxation time for 80/15/5/6 is much longer than that of 80/15/5/4 and 80/15/5/2 blends. Also, similar relaxation spectra were obtained for the 70/25/5/2 to 70/25/5/6 blends. According to Figure 4, it can be concluded that the relaxation time increases with the incorporation of nanoclay loading (2–6 wt %). The nanoclay initiates processes with long relaxation times, thus it can be detected very sensitively by

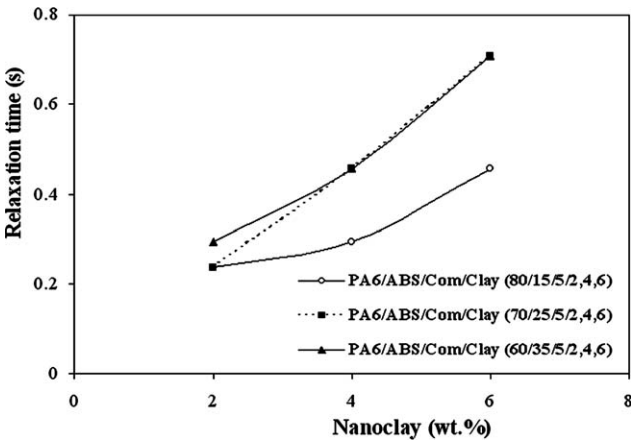

Figure 4 Dependence of the characteristic relaxation times as a function of the nanoclay for PA6/ABS/Com/Nanoclay blends at 245°C.

rheology.[36] This behavior implies that the polymer chains experience increased friction forces resulting in a delayed relaxation. Even higher relaxation time can be assigned to the nano-filled blends, indicating stronger filler–matrix interactions.[37] Also, the relaxation time behavior for all of the blends is similar to each other at steady ABS levels. Depending on relaxation times, the nanoclay particles are confined in one of the two phases, in both phases ,or can be restricted at the interface between the two polymers. Conversely, by increasing the ABS content (15–35 wt %) increases in relaxation times for all of the blends with steady nanoclay content occurred. It can be seen that the relaxation times of the dispersed droplets increase when the dispersed phase concentration increases. The relaxation time is directly proportional to the size of the dispersed phase.[38] Consequently, the increase of elasticity can be attributed to the form relaxation process of the dispersed phase droplets when slightly sheared.[24,25] When the dispersed phase content increases, the diameter of the dispersed phase increases and the relaxation process of the dispersed phase becomes extended, leading to an increase of the elastic modulus.[38] Also, the transition from the peak of the PA6 to the peak of the ABS implies increasing the miscibility and compatibility of the PA6/ABS blend components. In other words, when the relaxation time of the disperse phase increases, the plateau also increases, G' Figure 2, which was expected due to the increased elasticity levels. Moreover, the incorporation of nanoclay results in a broadened relaxation time spectrum and an increase in zero-shear viscosity (η_0) according to Carreau–Yasuda model as followed to eq. (4).[39–41]

$$\eta = (\eta_0 - \eta_\infty) \times (1 + (\lambda.x)^a)^{\frac{(n-1)}{a}} + \eta_\infty \qquad (4)$$

where η_0 and η_∞ are the zero-shear viscosity and infinite shear viscosity, respectively, and so a, n, and λ

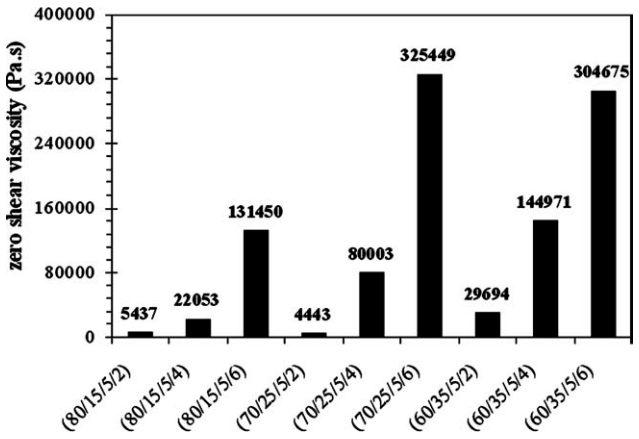

Figure 5 Comparison of the zero-shear viscosity for the PA6/ABS/Com/Nanoclay blends at 245°C.

is the width of the transition range between zero-shear viscosity and power law region, power law exponent, and relaxation time, respectively. The zero-shear viscosity between the dispersed phase and the matrix for all of the blends at 245°C is illustrated in Figure 5. As can be seen from Figure 5, the zero-shear viscosity values, η_0, were obtained by fitting the complex viscosity curve versus frequency using the Carreau–Yasuda model. The zero-shear viscosity was extracted in the terminal frequency region. It can be concluded that the zero-shear viscosity increases by increasing of the nanoclay and ABS loading. Conversely, as the content of nanoclay increased, the peak of the relaxation spectrum shifted to longer times and the shape of the spectrum became broader indicating a different relaxation mechanism. The slow relaxation was attributed to the rigidity of the polymer molecules, which restrict the chain mobility.[42] Therefore, the relaxation spectra of 60/35/5/6 blend is broader than other blends. The PA6/ABS/Com/Nanoclay (60/35/5/6) blend with a cocontinuous morphology usually exhibits a power-law-like relaxation of the elastic modulus at low frequencies. This is ascribed to the presence of domains with different characteristic length scales, resulting in a continuous relaxation time spectrum.[43,44] We concluded that in the nanocomposites, the relaxation time is delayed, and the orientation of the polymer chains should be easier than in the pure matrix.

Influence of nanoclay addition on morphology and rheological properties

It was demonstrated that the results of linear viscoelastic measurements can provide a great insight into understanding the correlation between the interfacial elasticity and the morphology of immiscible polymer blends. Figure 6(a)–(f) shows the relationship between phase morphology and rheological behavior for PA6/ABS/Com/Nanoclay blends at 245°C. As shown in Figure 6(a)–(f), the droplet-matrix and cocontinuous morphology are observed for the 80/15/5/2,4,6 and 60/35/5/2,4,6 blends, respectively. These observations confirm that the cocontinuous and droplet-matrix morphologies are responsible for the characteristic complex rheological behaviors mentioned above. Recently, several authors have observed the unexpected formation of cocontinuous morphologies in polymer blends filled with nanoclay.[45–48] Accordingly, it seems that the interfacial relaxation time is also dependent upon the relaxation time of the continuous phase.[35] This also confirms that the compatibility between PA6 matrix and ABS disperse phase is improved due to suppressing the coalescence of the droplets by increasing the nanoclay loading. The presence of nanoclay at the interface stabilizes the blend morphology by suppressing the coalescence of the droplets. Also, it was observed that the disperse phase droplets in 80/15/5/2,4,6 blends were approximately spherical whereas in the 60/35/5/2,4,6 blends were elongated disperse phase droplet toward cocontinues. This deformation of the disperse phase droplets, which is due to a better adhesion between the phases, could clarify the increase in relaxation time. Furthermore, the increase in relaxation time of PA6/ABS/Nanoclay blends by rising of the nanoclay explained with deformation of droplets and also by the physical interactions across the interface that cause to enhancement of elasticity.[49] The droplet sizes obtained by rheology and those obtained by morphology are in good agreement. Moreover, it was interesting to note that the results obtained from morphological observations and relaxation time spectrum measurements are in qualitative agreement. Also, it is concluded that the influence of the nanoclay loading on the morphology and rheology of the blends is related to its location in the blend. This interfacial tension reduction arises from the localization of the nanoclay at the interface and its nonhomogeneous distribution along the interface, suppressing the coalescence between the droplets, which is a role of a compatibilizer.[9] Conclusively, the immiscible polymer blends can be compatibilized with nanoclay. Also, the nanoclay changes the blend morphology by interfacial tension reduction due to the localization of the nanoclay at the interface and by the viscosity ratio change due to the selective localization by its affinity to a specific component in the blend. Hence, the addition of nanoclay in the role of a compatibilizer results in a decreased domain size of the dispersed phase, stabilization of the dispersed phase, and finally, an improved interfacial adhesion. Recently, nanoclay particles are used as compatibilizer for immiscible polymer blends due to its compatibilization effect. Consequently, the

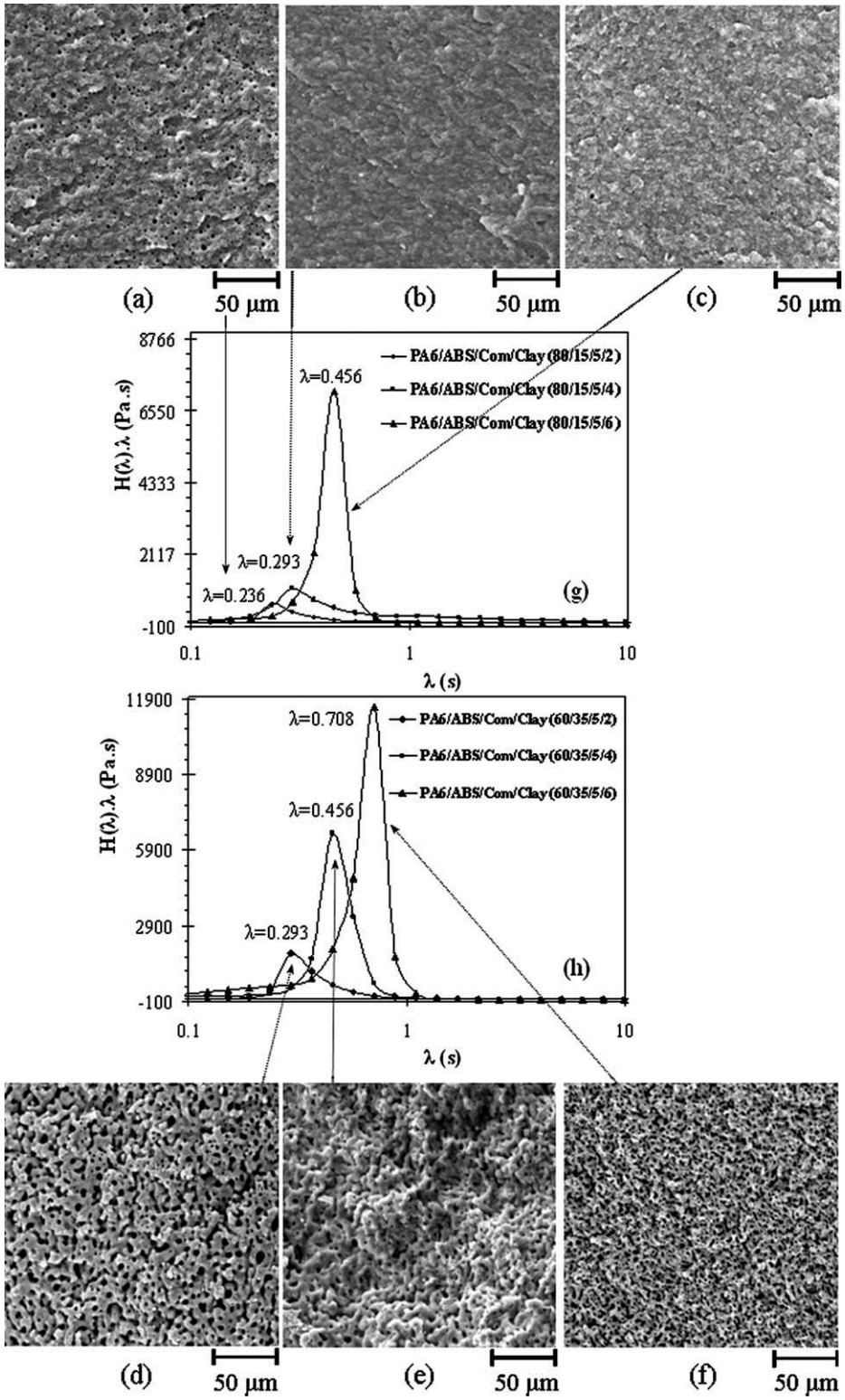

Figure 6 Comparison of the $H(\lambda)\lambda$ as a function of relaxation time and SEM images to represent the phase structures formed in the PA6/ABS/Com/Nanoclay blends.

finer morphologies with homogeneous particle dispersion were obtained. Accordingly, it seems that the interfacial relaxation time is also dependent upon the relaxation time of the continuous phase.

Nanoclay effects on interfacial relaxation time

If the amount of nanoclay within the dispersed droplet is increased, the deformability of the droplet filled with nanoclay is significantly reduced. On the

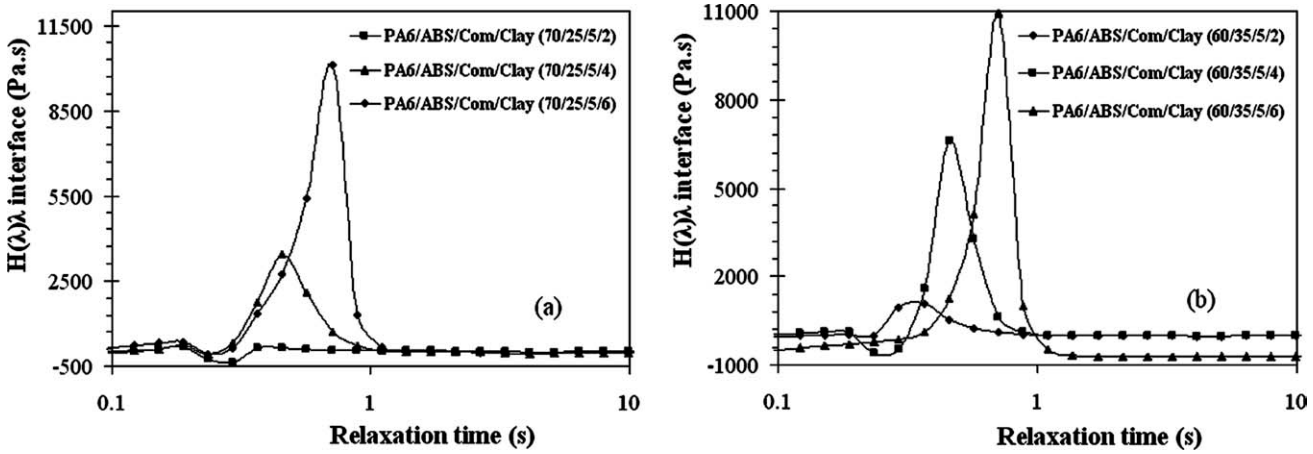

Figure 7 Interfacial relaxation time spectrum versus relaxation time for PA6/ABS/Com/Nanoclay blends at 245°C.

other hand, if the nanoclay is situated in the matrix, the size reduction effect is enhanced as the amount of nanoclay is increased.[12] This selective localization of the nanoclay results in a variation in the melt blend elasticity. A method suggested by Gramespacher and Meissner[23] consists of plotting the relaxation time spectrum $H(\lambda)$ λ versus λ and using the position of the maximum in the resulting curve as the relaxation time for the droplets.[50]

$$H(\lambda)\lambda_{\text{interface}} = H(\lambda)\lambda_{\text{nanocomposite}} - H(\lambda)\lambda_{\text{component}} \quad (5)$$

Gramespracher and Meissner suggested a simple linear mixing rule for $H(\lambda)\lambda_{\text{component}}$, which is defined as follows:

$$H(\lambda)\lambda_{\text{component}} = \varphi H(\lambda)\lambda + (1-\varphi)H(\lambda)\lambda_{PA6} \quad (6)$$

Substituting eq. (6) into eq. (5) then yields $H(\lambda)\lambda_{\text{component}}$:

$$H(\lambda)\lambda_{\text{interface}} = H(\lambda)\lambda_{\text{nanocomposite}} - \varphi.H(\lambda)\lambda_{ABS} - (1-\varphi)H(\lambda)\lambda_{PA6} \quad (7)$$

The resulting interfacial relaxation spectra for the blends are shown in Figure 7. All the blends show a single interfacial relaxation spectrum corresponding to the shape relaxation of drops. An alternative procedure to isolate the contribution of the interface has been evaluated here as well. In this approach, the contribution of the components is subtracted from the spectrum of the blend to get the interfacial relaxation spectrum.[50] This method is based on the assumption that the contributions of the different relaxation processes involved are additive.[50] The relaxation time at which the maximum occurs in the spectra of Figure 3 increases with increasing nanoclay, also the level of the maximum increases. Because higher nanoclay content implies smaller disperse phase droplets according to Figure 6 and consequently a strong interface, the spectrum should shift as observed. Corresponding to Figure 6, upon increasing nanoclay content, the peak height of $H(\lambda)\lambda_{\text{interface}}$ raised and relaxation time shifted to long-time region. The nanoclay localization in blend can be suggested from $H(\lambda)\lambda_{\text{interface}}$ as a function of λ diagram which nanoclay plates locate in the matrix, dispersed, or interphase. According to Figures 3 and 7, the amount of $H(\lambda)\lambda_{\text{interface}}$ is partially less than $H(\lambda)\lambda_{\text{nanocomposite}}$ so it can be suggested that the majority component of nanoclay is located in the interface. Because nanoclay plates is in the interface, so elastic behavior increases in low frequency by increasing nanoclay content. So because of being nonoclay in interface, the mobility of chains has been restricted and so resulted enhancement of elasticity in low frequency. This increased elasticity can be attributed to the relaxation time of disperse phase. In other words, this phenomenon causes the relaxation time very slightly shifted toward higher values in comparison with the blends with a smaller amount of nanoclay. Results show that the investigation of the relaxation time spectra of the nano-filled blends showed a distinct peak which could be related to the elastic response of the droplets and interface elasticity.

Influence of nanoclay on the relaxation modulus

The relaxation spectrum can be defined from the decomposition of the rheological functions in Maxwell modes and from the decomposition of the relaxation modulus in terms of exponential functions as follows[27]:

$$G(t) = \int_0^\infty H(\lambda)e^{-t/\lambda}\frac{d\lambda}{\lambda} \quad (8)$$

The stress relaxation modulus $G(t)$, in response to a low strain (10%) in the linear regime, is equal to the

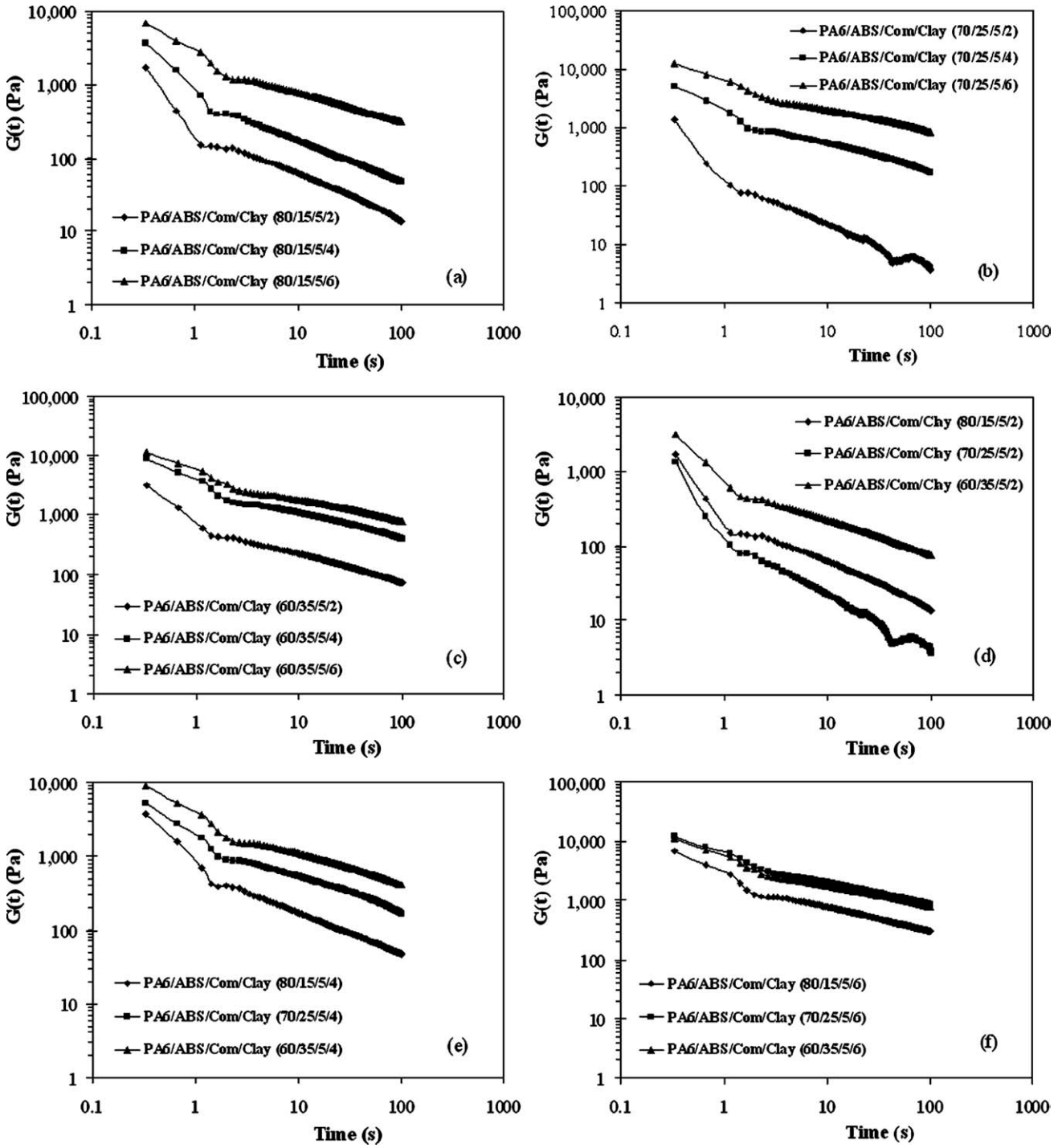

Figure 8 Relaxation modulus versus time of PA6/ABS/Com/Nanoclay blends of varying ABS and nanoclay contents at 245°C.

oscillatory response. The initial small-time response of $G(t)$ is equivalent to the high frequency response, and the long-time response is equal to the low frequency response. The relaxation modulus curve in the linear viscoelastic region has an exponential-like decay. In this case, Marrucci[51] proposed the following equation for investigation of the relaxation modulus at low frequency.

$$G(t) \cong G_p \tag{9}$$

where $G(t)$ is the relaxation modulus and G_P is the plateau modulus. According to eq. (9), the relaxation modulus enhanced with increasing the plateau modulus at low frequency domains. The effect of nanoclay addition on the variation of the relaxation modulus in response to a low strain (10%) in the

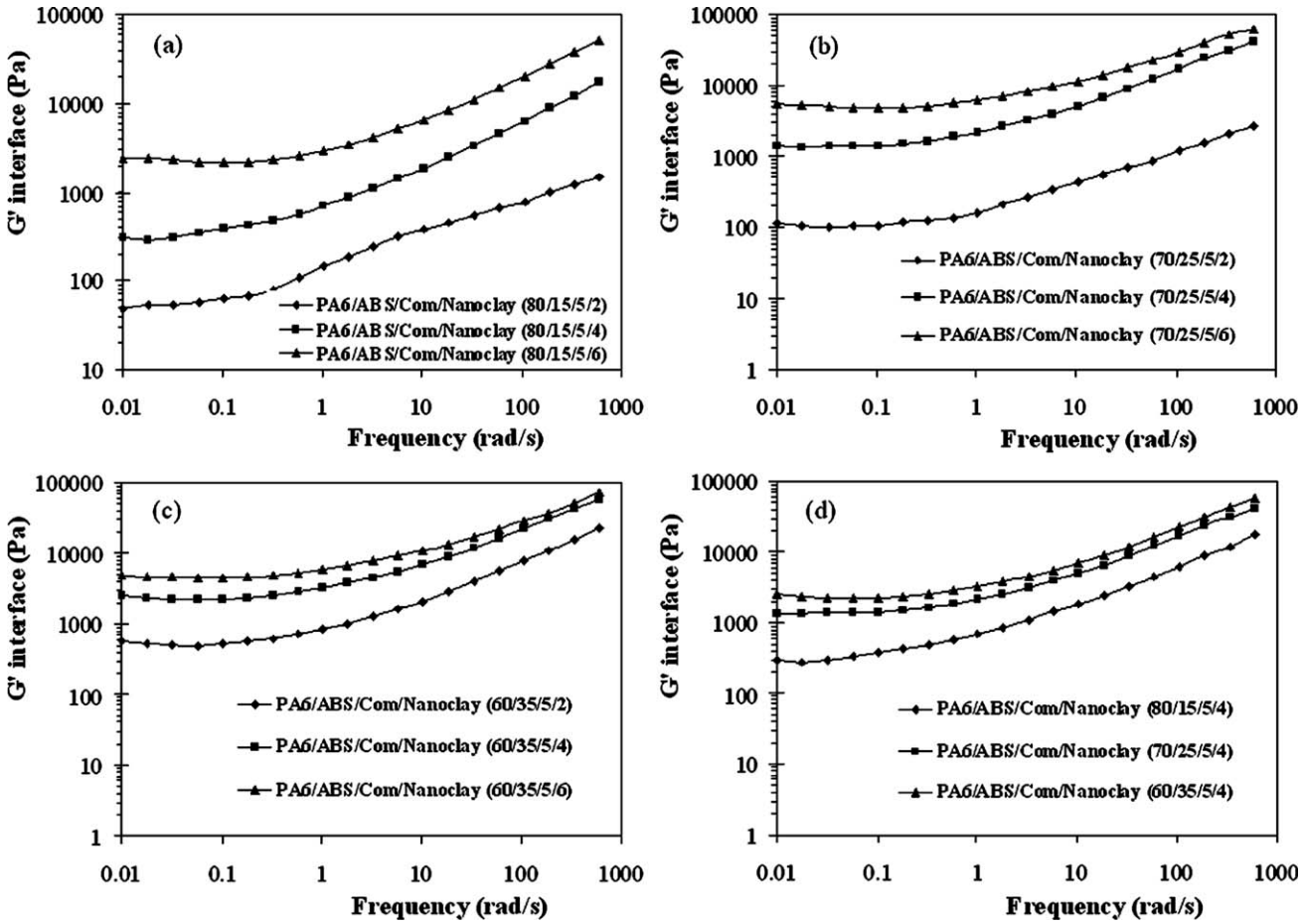

Figure 9 Interface modulus versus frequency for PA6/ABS/Com/Nanoclay blends at 245°C.

linear regime is shown in Figure 8. According to Figure 8, the slopes of $G(t)$ curves decrease by increasing nanoclay and ABS content, indicating that the relaxation time increases with the incorporation of nanoclay and ABS. We can observe that the nanoclay loading has significant influence on the storage modulus of the blends, so results increasing of plateau modulus, that corresponding to eq. (9), by increasing of G_P relaxation modulus have been raised. The relaxation modulus behavior was also enhanced by showing more solid-like characteristics by increasing nanoclay loading. Corresponding to Figure 8, all of the blends first exhibited quickly and then slow relaxation processes. It can be seen that the length of the plateau increases with increasing dispersed phase concentration due to larger deformations of the droplets. It can also be seen from Figures 6 and 8 that the slope of the plateau is declining when the nanoclay and dispersed phase content of the deformed droplet is increasing. Hence, two relaxation stages presented for all the blends: a first fast relaxation to 1 s, which can be related to the contribution of the pure phases; whereas a slower one, which was characterized by the presence of a plateau, which corresponds to the relaxation of the deformed droplets.[21] It can also be observed that, upon increasing dispersed phase content the slope of the plateau decreases,[21] indicating a slower relaxation when the size of the dispersed phase increases especial in the case of 60/35/5/6 blend. As, in immiscible polymer blends, the component polymers relax nearly alone in each phase.[22] On the other hand, the relaxation modulus increases with increasing amount of nanoclay added to the blend because the contribution of the interface increases with increasing nanoclay loading. For any fixed time, the $G(t)$ increases with increasing nanoclay loading, similar to that observed in the dynamic oscillatory shear measurements.

Influence of nanoclay on the interface modulus

In general, the dynamic storage modulus (G') of the immiscible polymer blend contains two interfacial contribution to the storage modulus is defined as follows:

$$G'_{\text{nanocomposite}} = G'_{\text{components}} + G_{\text{interface}'} \qquad (10)$$

The Gramespracher and Meissner[23] suggested a simple linear mixing rule for $G'_{\text{component}}$:

$$G'_{\text{components}} = \varphi G'_{ABS} + (1-\varphi)G'_{PA6} \quad (11)$$

Substituting eq. (11) into eq. (10) then yields $G'_{\text{component}}$:

$$G'_{\text{interface}} = G'_{\text{nanocomposite}} - \varphi G'_{ABS} - (1-\varphi)G'_{PA6} \quad (12)$$

where φ is the volume fraction of the dispersed phase, G'_{ABS} and G'_{PA6} are the storage modulus of dispersed phase and matrix, respectively. In this case, it can be considered that the ($G'_{\text{nanocomposite}}$) as contribution of intercalated nanoclay to the storage modulus can be studied in terms of the confinement effect ($G'_{\text{confinement}}$) and the interaction between the tactoids ($G'_{\text{interface}}$) effects, which result in the enhancement of G' at low frequency in comparison with G'_{matrix} the polymer matrix.[21,35] Where G' components and G' interface represent the modulus of the two components and of the phase interface, respectively. These interactions can result in the remarkable enhancement when the nanoclay loading is higher than a percolation threshold, which may lead to the considerable enhancement of low frequency elasticity.[52] The $G'_{\text{nanocomposite}}$ may be dominated by $G'_{\text{interface}}$ because the contribution of $G'_{\text{interface}}$ is much bigger than those of G'_{matrix} and $G'_{\text{confinement}}$ at low frequencies. The component polymers contribution is negligible at low frequencies, and therefore $G'_{\text{interface}}$ at low frequencies is not sensitive to choice of $G'_{\text{component}}$. The effect of nanoclay addition on the $G'_{\text{interface}}$ as a function of frequency is shown in Figure 9. As can be seen, the value of plateau interfacial elastic modulus is also considerably influenced by the presence of nanoclay loading. Increases at nanoclay weight fraction, confirming an enhanced interfacial contribution. According to Figure 9, the results confirm the enhancement in elasticity and formation of plateau at low frequency domains. On the other hand, the elasticity seems to provide a sensitive way to assess the cocontinuity in immiscible polymer blends. Hence, the interfacial elastic modulus of the blends measured at all of the frequencies provides further evidence of the morphological changes (Fig. 6). This deceleration in relaxation mechanism at low frequencies is reported often for a variety of nano-filled polymer melts.[53] As, interactions can also sharply increase when the nanoclay loading is above a percolation threshold, which may lead to the significant enhancement of low frequency $G'_{\text{interface}}$. In the literature, the plateau in G' exhibited by nanocomposites at lower frequencies above a critical concentration was often interpreted as the occurrence of a transition from a liquid-like to a solid-like behavior.[52] This solid-like behavior is characterized by the appearance of a plateau modulus at low frequencies corresponding to a enhancement of elasticity and the longest relaxation time. At high nanoclay loading, the contribution of the interphase was evidenced.

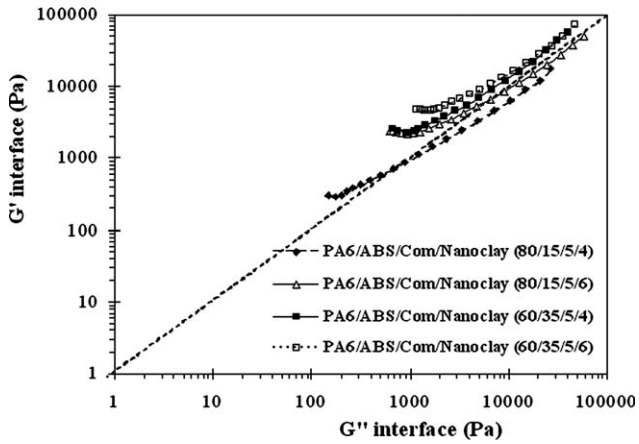

Figure 10 $G'_{\text{interface}}$ versus $G''_{\text{interface}}$ for the PA6/ABS/Com/Nanoclay blends at 245°C.

Han plot

Figure 10 represents a comparison of the curves of $G'_{\text{interface}}$ versus $G'_{\text{interface}}$ for different compositions of the PA6/ABS/Com/Nanoclay blends at 245°C to investigate the compatibility and alter of the microstructure in polymer blends.[54–57] It can be seen that the slope slightly decreases with the nanoclay and ABS content. Additionally, the curves indicated that the addition of nanoclay and ABS enhanced the elasticity of the blends and changed the microstructure. Therefore, the differences in the shapes of the curves that means the addition of nanoclay and ABS changed the melt behavior blends from viscose to elastic, and also altered morphological structure from disperse–matrix to cocontinuous in some of the blends. The change in overall behavior of $G'_{\text{interface}}$–$G''_{\text{interface}}$ plot of nanocomposites over 2 wt % nanoclay in many of the blends is the evidence of interparticle interactions. So with increasing the nanoclay loading elasticity increases and the phase morphology of system is going toward cocontinuous (60/35/5/2,4,6). From this result, it can be expected that the high elasticity justifies the compatibility of components. In addition, it was interesting to note that morphological observations and rheological measurements are in good agreement.

CONCLUSIONS

The purpose of this research was to study the influence of nanoclay on the rheological behavior of PA6/ABS/Nanoclay blends such as mechanism of relaxation time, interfacial relaxation time, relaxation modulus, interface modulus, and the relationship between the rheological behaviors of the blends and their morphologies was investigated. The melt

rheological analysis on PA6/ABS/Nanoclay blends was performed to obtain the linear viscoelastic behavior and to get information on the relaxation times of the blends, which are essential for a significant understanding of the increasing nanoclay effect on melt elasticity behavior. The main results obtained in this work are summarized as follows.

1. It can be concluded that the incorporation of nanoclay (2–6%) and ABS (15–35%) causes to increasing of relaxation time and zero-shear viscosity for all of the blends. On the other hand, the increase in relaxation time of PA6/ABS/Nanoclay blends by rising of the nanoclay explained with deformation of droplets and also by the physical interactions across the interface that causes to enhancement of elasticity. Moreover, the enhancement of elasticity can be attributed to the relaxation time of disperse phase. In other words, this phenomenon causes the relaxation time very slightly shifted toward higher values by increasing of the nanoclay loading.
2. The relaxation time spectrum caused by the interfacial tension of the droplets can be calculated by subtracting the contribution of the components from the global nanocomposite spectrum. Furthermore, the nanoclay localization in blend can be suggested from $H(\lambda)\lambda_{interface}$ as a function of λ diagram which nanoclay plates locate in matrix, dispersed, or interphase.
3. In addition, the slopes of $G(t)$ curves decrease by increasing nanoclay and ABS content, indicating that the relaxation time increases with the addition of nanoclay and ABS content.
4. Also, the value of plateau interfacial elastic modulus is also influenced considerably by the presence of the nanoclay. Increases at nanoclay weight fraction, confirming an enhanced interfacial contribution.

References

1. Kordjazi, Z.; Golshan-Ebrahimi, N. J Appl Polym Sci 2010, 116, 441.
2. He, X.; Yang, J.; Zhu, L.; Wang, B.; Sun, G.; Lv, P.; Phang, I. Y.; Liu, T. J Appl Polym Sci 2006, 102, 542.
3. Xu, G.; Chen, G.; Ma, Y.; Ke, Y.; Han, M. J Appl Polym Sci 2008, 108, 1501.
4. Gu, S. Y.; Ren, J.; Wang, Q. F. J Appl Polym Sci 2004, 91, 2427.
5. Li, J.; Zhou, C.; Wang, G.; Zhao, D. J Appl Polym Sci 2003, 89, 3609.
6. Ray, S. S.; Okamoto, K.; Okamoto, M. J Appl Polym Sci 2006, 102, 777.
7. Wagener, R.; Reisinger, T. J. G. Polymer 2003, 44, 7513.
8. Zhao, J.; Morgan, A. B.; Harris, J. D. Polymer 2005, 46, 8641.
9. Hong, J. S.; Kim, Y. K.; Ahn, K. H.; Lee, S. J.; Kim, C. Rheol Acta 2007, 46, 469.
10. Huitric, J.; Ville, J.; Médéric, P.; Moan, M.; Aubry, T. J Rheol 2009, 53, 1101.
11. Quansheng, S.; Meng, F.; Shimin, Z.; Jianming, J.; Mingshu, Y. Polym Int 2007, 56, 50.
12. Hong, J. S.; Namkung, H.; Ahn, K. H.; Lee, S. J.; Kim, C. Polymer 2006, 47, 3967.
13. Filippone, G.; Dintcheva, N. T.; Acierno, D.; La Mantia, F. P. Polymer 2008, 49, 1312.
14. Yamane, H.; Takahashi, M.; Hayashi, R.; Okamoto, K.; Kashihara, H.; Masuda, T. J Rheol 1998, 42, 567.
15. Okamoto, K.; Takahashi, M.; Yamane, H.; Kashihara, H.; Watanabe, H.; Masuda, T. J Rheol 1999, 43, 951.
16. Iza, M.; Bousmina, M. J Rheol 2000, 44, 1363.
17. Hayashi, R.; Takahashi, M.; Kajihara, T.; Yamane, H. J Rheol 2001, 45, 627.
18. Jansseune, T.; Moldenaers, P.; Mewis, J. J Rheol 2003, 47, 829.
19. Ansari, M.; Haghtalab, A.; Semsarzadeh, M. A. Rheol Acta 2006, 46, 983.
20. Mechbal, N.; Bousmina, M. Macromolecules 2007, 40, 967.
21. Yee, M.; Souza, A. M. C.; Valera, T. S.; Demarquette, N. R. Rheol Acta 2009, 48, 527.
22. Takahashi, M.; Paulo, H. P.; Macaúbas, K. O.; Jinnai, H.; Nishikawa, Y. Polymer 2007, 48, 2371.
23. Gramespacher, H.; Meissner, J. J Rheol 1992, 36, 1127.
24. Bousmina, M.; Muller, R. J Rheol 1993, 37, 663.
25. Lacroix, C.; Bousmina, M.; Carreau, P. J.; Favis, B. D.; Michel, A. Polymer 1996, 37, 2939.
26. Honerkamp, J.; Weese, J. Rheol Acta 1993, 32, 65.
27. Ferry, J. D.; Viscoelastic Properties of Polymers; Wiley: New York, 1980.
28. Carreau, P. J.; De Kee, D.; Chhabra, R. P.; Rheology of Polymer Systems: Principles and Applications; Hanser: Munich, 1997.
29. Tschoegle, N. W. The Phenomenological Theory of Linear Viscoelastic Behavior; Spinger-Verlag: Berlin, 1989.
30. Pötschke, P.; Fornes, T. D.; Paul, D. R. Polymer 2002, 43, 3247.
31. Vermant, J.; Ceccia, S.; Dolgovskij, M. K.; Maffettone, P. L.; Macosko, C. W. J Rheol 2007, 51, 429.
32. Fornes, T. D.; Yoon, P. J.; Keskkula, H; Paul, D. R. Polymer 2001, 42, 9929.
33. Durmus, A.; Kasgoz, A.; Macosko, C. W. Polymer 2007, 48, 4492.
34. Kim, H. B.; Choi, J. S.; Lee, C. H.; Lim, S. T.; Jhon, M. S.; Choi, H. Eur Polym J 2005, 41, 679.
35. Lee, H. M.; Parka, O. O. J Rheol 1994, 38, 1405.
36. Kovács, J.; Dominkovics, Z.; Vörös, G.; Pukánszky, B. Macromol Symp 2008, 267, 47.
37. Kelarakis, A.; Emmanouel, P. G.; Yoon, K. Polymer 2007, 48, 7567.
38. Patrícia, S. C.; Yee, M.; Demarquette, N. R. Polymer 2005, 46, 2610.
39. Stadler, R.; Freitas, L. D. L. Colloid Polym Sci 1988, 266, 1102.
40. Sperling, L. H. Introduction to Physical Polymer Science; Wiley: New York, 1992.
41. Caia, H.; Ait-Kadi, A.; Brisson, J. Polymer 2003, 44, 1481.
42. Nandan, B.; Kandpal, L. D.; Mathur, G. N. J Polym Sci B: Polym Phys 2004, 42, 1548.
43. Vinckier, I.; Laun, H. M. Rheol Acta 1999, 38, 274.
44. Krishnamoorti, R.; Yurekli, K. Curr Opin Colloid Interface Sci 2001, 6, 464.
45. Ly, Y.; Shimizu, H. Polymer 2004, 45, 7381.
46. Ly, Y.; Shimizu, H. Macromol Rapid Commun 2005, 26, 710.
47. Wu, D.; Zhou, C.; Zhang, M. J Appl Polym Sci 2006, 102, 3628.
48. Ray, S. S.; Bandyopadhyay, J.; Bousmina, M. Macromol Mater Eng 2007, 292, 729.
49. Silva, J. M.; Machado, A. V.; Moldenaers, P.; Maia, J. M. Korea–Australia Rheol J 2010, 22, 21.
50. Vinckier, I.; Moldenaers, P.; Mewis, J. J Rheol 1996, 40, 613.
51. Marrucci, M. J Polym Sci B: Polym Phys 1985, 23, 159.
52. Wu, D.; Zhou, C.; Hong, Z.; Mao, D.; Bian, Z. Eur Polym Mater 2005, 41, 2199.
53. Sarvestani, S. A. Eur Polym Mater 2008, 44, 263.
54. Krache, R.; Benachour, D.; Pötschke, P. J Appl Polym Sci 2004, 94, 1976.
55. Chaung, H. K.; Han, C. D. J Appl Polym Sci 1984, 29, 2205.
56. Han, C. D.; Yang, H. H. J Appl Polym Sci 1987, 33, 1199.
57. Han, C. D. J Appl Polym Sci 1988, 35, 167.